Molecular Biology of the Cell
Vol. 10, 741–756, March 1999

Interaction of the Doa4 Deubiquitinating Enzyme with the Yeast 26S Proteasome

Feroz R. Papa, Alexander Y. Amerik, and Mark Hochstrasser*

Department of Biochemistry and Molecular Biology, University of Chicago, Chicago, Illinois 60637

Submitted September 23, 1998; Accepted December 17, 1998
Monitoring Editor: Peter Walter

The *Saccharomyces cerevisiae* Doa4 deubiquitinating enzyme is required for the rapid degradation of protein substrates of the ubiquitin–proteasome pathway. Previous work suggested that Doa4 functions late in the pathway, possibly by deubiquitinating (poly)-ubiquitin-substrate intermediates associated with the 26S proteasome. We now provide evidence for physical and functional interaction between Doa4 and the proteasome. Genetic interaction is indicated by the mutual enhancement of defects associated with a deletion of *DOA4* or a proteasome mutation when the two mutations are combined. Physical association of Doa4 and the proteasome was investigated with a new yeast 26S proteasome purification procedure, by which we find that a sizeable fraction of Doa4 copurifies with the protease. Another yeast deubiquitinating enzyme, Ubp5, which is related in sequence to Doa4 but cannot substitute for it even when overproduced, does not associate with the proteasome. *DOA4-UBP5* chimeras were made by a novel PCR/yeast recombination method and used to identify an N-terminal 310-residue domain of Doa4 that, when appended to the catalytic domain of Ubp5, conferred Doa4 function, consistent with Ubp enzymes having a modular architecture. Unlike Ubp5, a functional Doa4-Ubp5 chimera associates with the proteasome, suggesting that proteasome binding is important for Doa4 function. Together, these data support a model in which Doa4 promotes proteolysis through removal of ubiquitin from proteolytic intermediates on the proteasome before or after initiation of substrate breakdown.

INTRODUCTION

Ubiquitin is a conserved 76-residue polypeptide whose covalent attachment to various proteins mediates numerous cellular processes (Wilkinson, 1995; Hochstrasser, 1996; Pickart, 1997; Varshavsky, 1997). In ubiquitin–protein conjugates, one or more substrate lysine side chains are linked by an amide (isopeptide) bond with the C terminus of ubiquitin. For efficient targeting to the 26S proteasome, formation of a polyubiquitin chain on the substrate is generally required. Ubiquitination of proteins can be reversed through the action of deubiquitinating enzymes (DUBs), which hydrolyze the linkage between ubiquitin and substrate (Wilkinson and Hochstrasser, 1998). DUBs are specialized thiol proteases that fall into two sequence classes, the larger of which is the ubiquitin-specific processing protease (UBP) class. There are 16 apparent UBPs encoded by the yeast *Saccharomyces cerevisiae* genome (Hochstrasser, 1996). These proteins are largely divergent in primary sequence except in two short motifs, the Cys and His boxes, which are likely to form part of the active site (Baker *et al.*, 1992; Papa and Hochstrasser, 1993). Many *UBP* genes have been identified only by these signature motifs, and the cellular functions of most of the UBPs have not yet been discovered (Hochstrasser, 1996; Wilkinson and Hochstrasser, 1998). An exception is Ubp14, which was recently shown (Amerik *et al.*, 1997) to be the functional homologue of the mammalian enzyme isopeptidase T (Falquet *et al.*, 1995; Wilkinson *et al.*, 1995). Both isopeptidase T and Ubp14 disassemble free polyubiquitin chains in vitro. Loss of Ubp14 leads to an accumulation of free polyubiquitin chains in vivo and inhibition of ubiquitin-dependent proteolysis, apparently through compe-

* Corresponding author. E-mail address: hoc1@midway.uchicago.edu.

tition by free chains for polyubiquitin-substrate binding sites on the proteasome (Amerik *et al.*, 1997).

The 26S proteasome is a multisubunit complex composed of a 20S catalytic core and a pair of 19S regulatory subcomplexes (Coux *et al.*, 1996; Hilt and Wolf, 1996; Baumeister *et al.*, 1998). The 19S regulatory particle, which is also referred to as PA700 (Ma *et al.*, 1994) or the μ particle (Udvardy, 1993), confers ATP dependence and ubiquitin dependence on protein degradation by the 20S proteasome. Destruction of proteins by the proteasome is processive and results in peptides averaging 7–12 residues in length (Akopian *et al.*, 1997). Ubiquitin itself appears to escape degradation and is recycled through the action of DUBs that act in concert with the proteasome. Consistent with this idea, ubiquitin isopeptidase activity has been shown to cofractionate with 26S proteasomes (Eytan *et al.*, 1993; Yoshimura *et al.*, 1993). Recently, a distinct isopeptidase activity that resides in the 19S complex was described (Lam *et al.*, 1997). In none of these examples is the identity of the DUB(s) known.

A focus of our work has been the yeast DOA (degradation of alpha 2) pathway, which targets the MATα2 transcriptional repressor for destruction (Hochstrasser *et al.*, 1995). DOA pathway proteins include ubiquitin-conjugating enzymes (Chen *et al.*, 1993), proteasomal subunits (Chen and Hochstrasser, 1995), and a deubiquitinating enzyme (Papa and Hochstrasser, 1993). This last enzyme, called Doa4/Ubp4, is central to the degradation of not only the α2 protein but also many other substrates of the ubiquitin-dependent proteolytic system. Mutant *doa4*Δ cells also accumulate small (poly)ubiquitinated species, which were postulated to be modified peptide remnants resulting from extensive degradation of ubiquitinated substrates by the proteasome. For these and other reasons, it was proposed that Doa4, like the proteasome, functions late in the ubiquitin pathway (Papa and Hochstrasser, 1993).

We show here that accumulation of these ubiquitinated species is indeed dependent at least in part on proteasomal action because a mutation in a proteasomal subunit gene, *DOA3*, largely suppresses their generation. Close association between proteasome and Doa4 activities was corroborated by biochemical analysis, which showed that a large fraction of Doa4 protein is associated with 26S proteasomes. We also describe a structure–function analysis of Doa4, with the aim of identifying regions in Doa4 that help specify its unique functional properties. A Doa4 "specificity element" was localized to the N-terminal 310 residues of the protein, and we show that this element contributes to Doa4 association with the proteasome. These results are consistent with a model in which one of the functions of Doa4 is the disassembly or removal of ubiquitin chains from substrates targeted to the 26S proteasome complex.

MATERIALS AND METHODS

Growth and Manipulation of Yeast and Bacteria

Yeast-rich and minimal media were prepared as described, and standard genetic methods were used (Ausubel *et al.*, 1989). The *Escherichia coli* strains used were MC1061 and JM101, and standard techniques were used for recombinant DNA work (Ausubel *et al.*, 1989).

Yeast Strain Constructions

All strains were congenic with the haploid strains MHY500 (*MAT***a** *his3-*Δ*200 leu2–3,112 ura3–52 lys2–801 trp1–1*) or MHY501 (*MAT*α *his3-*Δ*200 leu2–3,112 ura3–52 lys2–801 trp1–1*) or diploid strain MHY606 (*MAT***a**/*MAT*α *his3-*Δ*200/his3-*Δ*200 leu2–3,112/leu2–3,112 ura3–52/ura3–52 lys2–801/lys2–801 trp1–1/rp1–1*) (Chen *et al.*, 1993; Papa and Hochstrasser, 1993). The *doa4*Δ*::HIS3* strains MHY622 and MHY623 was described previously (Papa and Hochstrasser, 1993) as was the *doa3–1* strain MH16F9–1b (Chen and Hochstrasser, 1995). MHY623 and MH16F9–1b were mated, and the resulting double heterozygote was used to generate *doa4*Δ *doa3–1* haploid segregants. Strain MHY832 (*MAT***a** *his3-*Δ*200 leu2–3,112 ura3–52 lys2–801 trp1–1 doa4-*Δ*1::LEU2 pep4::HIS3*) was made by transforming MHY622 with a *pep4::HIS3* disruption allele (Woolford *et al.*, 1986). MHY905 was derived from MHY622 by chromosomal integration of a *Deg1-lacZ* reporter (Hochstrasser and Varshavsky, 1990).

A heterozygous *ubp5*Δ gene disruption was constructed in strain MHY606 by integrating a *HIS3* gene cassette with *UBP5* flanking sequences at the *UBP5* chromosomal locus. This resulted in replacement of the *UBP5* sequence between the two *Bgl*II sites (codons 442–716) by the *HIS3* gene, which was oriented in the same direction as *UBP5*. The insertion was confirmed by Southern DNA hybridization analysis. Haploid *ubp5*Δ mutants MHY662 (**a**) and MHY663 (α) were derived from the heterozygote by sporulation, tetrad dissection, and identification of histidine prototrophs.

Epitope-tagging of Proteins and Immunoblotting Methods

The coding sequence for three tandem hemagglutinin (HA) epitopes was amplified by a PCR from a plasmid template (Tyers *et al.*, 1992). The PCR fragment had *Bam*HI sites added at either end that were used to clone the fragment in frame into the unique *DOA4 Bgl*II site. An additional single HA coding sequence was placed at the 3′-end of the *DOA4* open reading frame (ORF) by a two-step PCR-mediated mutagenesis procedure (Ausubel *et al.*, 1989). The twice-modified *DOA4* gene was cloned into the low-copy YCplac33 vector, yielding pDOA4–8(HA), and into the high-copy vector YEplac195 (Gietz and Sugino, 1988). The ability of pDOA4–8(HA) to provide full Doa4 function was confirmed by rescue of the sporulation defect of a homozygous *doa4*Δ*/doa4*Δ diploid and restoration of normal *Deg1-*βgal degradation in *doa4*Δ haploid cells.

A 4.2-kb *Pst*I–*Hin*dIII fragment containing the *UBP5* gene was subcloned from λ clone 70459 (obtained from the American Type Culture Collection) into YEplac195 and was modified at the 3′-end of the ORF by PCR-mediated insertional mutagenesis with an oligonucleotide encoding three HA epitopes. The tagged enzyme was active in a deubiquitination assay using a ubiquitin–β-galactosidase fusion protein (Ub-M-βgal) expressed in *E. coli* (Papa and Hochstrasser, 1993).

To detect HA-tagged proteins, proteins were electrophoresed through 10% SDS-polyacrylamide gels and blotted onto nitrocellulose filters. The filters were blocked with 5% nonfat milk/Tris-buffered saline (TBS)-Tween 0.1% (Tris-HCl, pH 8.0, 150 mM NaCl, 0.1% Tween-20) and incubated with a mouse monoclonal antibody

against the HA epitope (12CA5; Babco Inc., Berkeley, CA) at a 1:1000 dilution in 1% nonfat milk/TBS-Tween 0.1% for 1 h, followed by three 10 min washes with 1% nonfat milk/TBS-Tween 0.1%. The blot was then probed with an anti-mouse immunoglobulin G + immunoglobulin M HRP-conjugated antibody (Boehringer Mannheim, Indianapolis, IN) at a 1:4000 dilution in 1% nonfat milk/TBS-Tween 0.1% for 1 h. After four more washes, the blot was washed in TBS for 10 min. Antibody binding was detected using enhanced chemiluminescence reagents from Amersham (Buckinghamshire, UK).

20S proteasome subunits and Cim5 were detected using the same protocol as used for HA-tagged proteins, except that the primary antibodies were used at 1:2000 dilutions (both gifts of K. Tanaka, The Tokyo Metropolitan Institute of Medical Science and CREST, Japan Science and Technology Corp.). Ubiquitin and ubiquitin–protein conjugates were detected using a polyclonal antibody from East Acres Biologicals (Southbridge, MA) as described previously (Papa and Hochstrasser, 1993). An anti-rabbit secondary immunoglobulin G HRP-conjugate antibody (Amersham) was used at 1:4000 dilution for detection of antibody binding to Cim5, 20S proteasome, and ubiquitin.

Purification of Yeast 26S Proteasomes

Cultures of *doa4*Δ *pep4* cells (MHY832; 3.5 l) harboring pDOA4–8(HA) were grown in minimal media lacking uracil to OD_{600} = 1–2 and collected by centrifugation for 10 min at 4000 rpm at 4°C, washed in 300 ml of ice-cold water, and resuspended in 150 ml of SCE buffer (1 M sorbitol, 100 mM sodium acetate, pH 7.2, 60 mM Na_2EDTA). Four hundred microliters of β-glucuronidase (46,000 U) (Sigma, St. Louis, MO) were added to the cell suspension and incubated for 1 h at 30°C with gentle shaking. Spheroplasts were collected by centrifugation (Sorvall, Newtown, CT; GSA rotor; 3000 rpm, 3 min at 4°C), and washed three times with 200 ml of 1 M sorbitol, each time collecting the spheroplasts gently by centrifugation at 3000 rpm for 3 min at 4°C. The spheroplast pellet was resuspended in 8 ml of cold 26S buffer (20 mM Tris-HCl, pH 7.5, 20 mM potassium acetate, 5 mM $MgCl_2$, 1 mM dithiothreitol, 2 mM ATP, 20% glycerol) to which pepstatin A was added to 10 μg/ml. The resuspended pellet was sonicated using a microtip in 30-s intervals interrupted by 30-s incubations on ice. Two low-speed centrifugations (20,000 × *g*; 20 min) were performed to clear debris and unlysed cells. The supernatant was then subjected to a 100,000 × *g* spin in a Beckman Instruments (Palo Alto, CA) Ti 70 rotor for 40 min at 4°C.

The supernatant was loaded using a 10 ml Superloop (Pharmacia, Piscataway, NJ) onto a Sephacryl S-400 gel filtration column (Pharmacia, 2.5 cm × 100 cm XK 26/100 column) that had been equilibrated in 26S buffer. The resin had been packed in water using a fast protein liquid chromatography system (FPLC) according to the manufacturer's instructions (Pharmacia). This and all subsequent chromatography steps were performed at 4°C. The flow rate was 0.5 ml/min, and 6.5 ml fractions were collected. A_{280} readings were obtained with an on-line spectrophotometer (Pharmacia). Fractions containing peptidase activity (see below) from the S-400 fractionation were pooled and loaded using a 50 ml Superloop onto an FPLC Mono Q HR (5/5) column (Pharmacia) in 26S Buffer at 1 ml/min, at a back-pressure of 4.5 MPa. The column elution rate was 0.5 ml/min. The eluting buffer was buffer B (26S buffer + 0.8 M NaCl). From t = 0 to t = 10 min, the column was washed with 26S Buffer. A linear salt gradient from t = 10 min (0% buffer B) to t = 40 min (100% buffer B) was generated followed by a 10 min plateau in buffer B. Finally, the column was washed with 26S buffer until t = 70 min; 0.5 ml fractions were collected. Fractions containing peptidase activity were pooled and concentrated to 0.3 ml using a 10-kDa cutoff Microcon concentrator (Amicon, Beverly, MA) with one change of 26S buffer (0.5 ml), which also served as a desalting step (performed at 4°C). The concentrated proteins were loaded onto an FPLC Superose 6 HR (10/30) column (Pharmacia) equilibrated in 26S buffer, and elution was continued in 26S buffer at 0.15 ml/min. Fractions (0.3 ml) were analyzed for peptidase activity and ubiquitin–lysozyme conjugate degrading activity. The most active fractions were pooled. Protein concentrations were determined using the BCA reagent from Pierce (Rockford, IL).

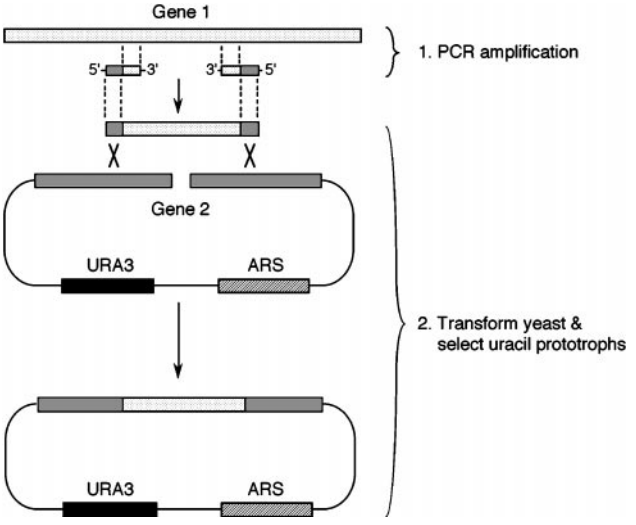

Figure 1. Outline of the PCR-based in vivo gap repair procedure (PCR–GR).

Peptidase and Ubiquitinated Lysozyme Degradation Assays

Peptidase activity was measured using the fluorigenic substrate *N*-succinyl-Leu-Leu-Val-Tyr-7-amido-4-methylcoumarin (suc-LLVY-AMC) (Sigma). A small amount of protein (20–50 μl) was added to 200 μl of assay buffer (50 mM Tris-HCl, pH 8.0, 1 mM β-mercaptoethanol, 50 μM suc-LLVY-AMC), and incubation was performed for 10–15 min at 37°C. The reaction was quenched by adding 2 ml of stop buffer (100 mM Tris-HCl, pH 10.0, 0.625% SDS). Reaction products were analyzed on a Perkin Elmer-Cetus Luminometer (Norwalk, CT) (absorption at 380 nm, emission at 460 nm) using a 1-s integration time. Measurement of polyubiquitinated lysozyme degradation (Hoffman *et al.*, 1992) was performed in a total volume of 100 μl, using 50 μl of Superose 6 fraction or an equal amount of 26S buffer. For reactions with an ATP regeneration system, 5 mM ATP, 50 μg/ml creatine kinase, and 50 mM creatine phosphate were added. For reactions depleted of ATP, 25 μg/ml hexokinase and 25 mM glucose were added. The reactions were brought to 87 μl with 26S buffer and preincubated at 32°C for 10 min; 13 μl of ubiquitinated [^{125}I]-lysozyme (a gift of Q. Deveraux and M. Rechsteiner, Department of Biochemistry, University of Utah) were then added, and the reaction was allowed to proceed for 45 min at 37°C, at which point 800 μl of an ice-cold solution of 2.5% (wt/vol) bovine serum albumin (Sigma) + 0.75% (wt/vol) lysozyme were added along with 100 μl of ice-cold 100% trichloroacetic acid. Reactions were precipitated on ice for 30 min and centrifuged at 14,000 × *g* for 20 min. Five hundred microliters of the supernatant were transferred into a new tube, and radioactivity in both supernatant and precipitate was counted in a γ-counter for 20 min.

Gene Fusion by PCR and Homologous Recombination in Yeast

We developed a method to fuse two genes (here, *DOA4* and *UBP5*) at any desired sequence without the need for compatible restriction enzyme sites at the fusion junction (Figure 1). A fragment of gene 1

(*UBP5*) was amplified by PCR using forward and reverse primers that both had bipartite sequences: 16–18 nucleotides (nt) of gene 1 sequences at the 3′ ends for annealing to gene 1, and 40–45 nt 5′ extensions derived from gene 2 (*DOA4*) sequences. The fusion junctions between genes 1 and 2 are therefore built into the PCR primers. For the PCR template, either a purified gene 1 fragment or a plasmid containing gene 1 that lacked a yeast replication origin was used. Gene 2, contained on a yeast–*E. coli* shuttle vector, was cut at a unique restriction site situated anywhere within the region of gene 2 that was to be replaced by the gene 1 fragment. Linear plasmids without telomeres are unstable in yeast, but if a DNA fragment bearing sequence homology to both sides of the gap site in a digested plasmid recombines with the gapped plasmid in vivo, a stable circular plasmid is generated. Homologous recombination rates in yeast are very high, and we found that plasmid gap repair was very efficient even when the length of the sequences at the ends of the PCR fragment that matched those in the gapped plasmid was only 40–45 bp (Baudin *et al.*, 1993).

Typically, 0.5 μg of the unpurified gapped gene 2-containing plasmid and 20% of the PCR reaction were cotransformed into a strain of *S. cerevisiae* auxotrophic for the nutritional marker encoded by the plasmid (Muhlrad *et al.*, 1992). We routinely obtained 50–100 times more colonies when the PCR fragment was included than when it was not. The false positive rate with a gapped plasmid restricted at two different sites was <5%. Recombinant plasmids were identified by yeast colony PCR and were then recovered in *E. coli* for restriction enzyme analysis and DNA sequencing. All plasmids that we identified as potential recombinants by yeast colony PCR had the correct fusion joints based on both restriction analysis and DNA sequencing. As an example, construction of *DOA4-UBP5* chimera 2 (see Figure 8) is described; other constructs were made similarly. The chimeric *DOA4-UBP5* construct 1 (made by standard cloning methods) was linearized by digestion of the *Sac*I and *Pst*I sites in the polylinker upstream of the *DOA4* insert. The sequence (~1 kb) upstream of the *UBP5* ORF was amplified by PCR from a plasmid containing *UBP5*. The upstream primer contained a 45-nt 5′ extension that was identical to a sequence upstream of the polylinker in construct 1. The downstream primer had a 45-nt 5′ extension that matched a *DOA4* sequence near the 5′ end of the *DOA4* ORF in its noncoding strand. The PCR fragment and *Sac*I/*Pst*I-digested *DOA4-UBP5* construct 1 were used for transformation. Sequencing of the resulting plasmids showed they had the expected exchange of the *UBP5* promoter for the *DOA4* promoter.

The PCR-based gap repair (GR) method is rapid and efficient and requires no in vitro mutagenesis or ligations. It can be used to recombine DNA elements from any organism as long as one of the DNA segments is carried on a plasmid harboring a yeast replication origin and selectable marker. Homologous recombination and gap repair to make recombinant plasmids in yeast was first described by Ma *et al.* (1987), and it has been used to recover PCR-generated fragments with *p53* alleles in yeast (Flaman *et al.*, 1995). The use of bipartite PCR primers to define precise fusion joints, as described here, provides a useful extension of these techniques.

RESULTS

Genetic Interaction of doa4Δ and doa3-1

As a first step toward evaluating whether Doa4 can associate with the proteasome, we investigated the effects of combining a deletion of the nonessential *DOA4* gene with a partial loss-of-function mutation in one of the essential 20S proteasome subunit genes, *DOA3/PRE2/PRG1* (Chen and Hochstrasser, 1995). If Doa4 functions in the proteasomal pathway, then mutant *doa3-1* cells, in which the catalytic core of the proteasome is compromised, might be sensitized to loss of the deubiquitinating enzyme and vice versa. We have found that *doa4Δ* spores arising from a sporulated *doa4Δ/DOA4* heterozygous diploid have a spore viability/germination defect that becomes more severe with extended incubation under sporulation conditions. Sporulation for 3 d at 30°C resulted in ~30% of *doa4Δ* spores failing to germinate. Strikingly, with the *doa3-1/+ doa4Δ/+* double heterozygote, which sporulated normally, no germination of *doa4Δ* spores was observed even when the spore carried a wild-type *DOA3* gene (nine full tetrads). This unusual germination defect was circumvented if the double heterozygote carried a low-copy *DOA4* plasmid, pDOA4-8, when it was sporulated. The pDOA4-8 plasmid could be lost from the *doa3-1 doa4Δ* segregants at 30°C, demonstrating that the double mutant was viable; however, *doa3-1 doa4Δ* cells grew much slower than either single mutant, and they failed to form colonies at 35°C, a temperature that allowed growth of both single mutants (Figure 2A). These mutual synthetic enhancement effects suggest that Doa4 and proteasome activities are functionally linked.

Mutant *doa4Δ* cells accumulate (poly)ubiquitinated species that are slightly larger than ubiquitin and ubiquitin multimers; these species might represent ubiquitin or ubiquitin chains attached to small remnant peptides derived from the hydrolysis of ubiquitinated proteins by the proteasome (Papa and Hochstrasser, 1993). If this were true, then mutational impairment of the proteasome in *doa4Δ* cells might suppress the accumulation of these conjugates. Antiubiquitin immunoblot analysis of extracts from *doa3-1 doa4Δ* cells (Figure 2B) demonstrated that the level of the low molecular mass conjugates was indeed greatly reduced relative to the *doa4Δ* single mutant; the residual accumulation might be attributable to the leaky nature of the *doa3-1* mutation. These data support the possibility that Doa4 and proteasome activities are closely coupled.

Association of Doa4 with 26S Proteasomes

The genetic data detailed above suggested that Doa4 might associate with or even be a component of the yeast 26 proteasome. To examine these ideas, a purification procedure for yeast 26S proteasomes was developed that yielded active enzyme of high purity. Purification of 26S proteasomes from yeast has proven to be more difficult than from other sources (Fischer *et al.*, 1994; Fujimuro *et al.*, 1998). For our purification, we followed cleavage of a fluorigenic proteasome substrate, suc-LLVY-AMC, to identify proteasome-containing fractions through different chromatographic steps, and a fully functional HA epitope-tagged Doa4 derivative was used in place of the wild-type protein to follow the partitioning of Doa4 throughout the purification using Western immunoblot analysis with an

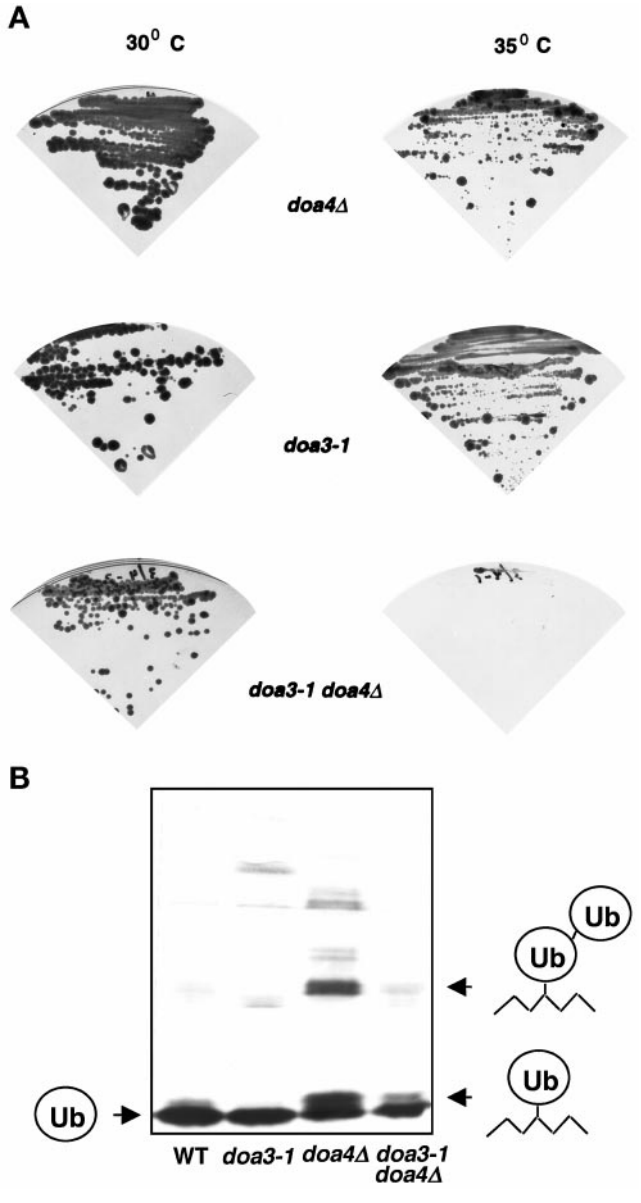

Figure 2. Genetic interaction between *doa4*Δ and *doa3*. (A) Enhanced growth defect of a *doa3-1 doa4*Δ double mutant. Doubly mutant *doa3-1 doa4*Δ cells, as well as the corresponding single mutants, were grown at 30°C and 35°C for one week. The wild-type parents grow equally well at both temperatures. (B) Suppression of the low molecular mass ubiquitin conjugates found in *doa4*Δ cells by impairment of the proteasome. Extracts from exponentially growing wild-type, *doa3-1*, *doa4*Δ, and *doa3-1 doa4*Δ cells were separated on an 18% polyacrylamide gel, blotted to a polyvinylidene difluoride membrane, and probed with an affinity-purified antiubiquitin antibody (a gift of Cecile Pickart, Department of Biochemistry, School of Public Health, Johns Hopkins University, Baltimore, MD). The positions of ubiquitin and the mono-ubiquitinated and di-ubiquitinated conjugates specific to *doa4* cells are indicated.

anti-HA monoclonal antibody. A doublet of bands at ~110 kDa is observed in HA-Doa4–expressing cells but not in cells expressing the untagged protein. In most experiments, we purified proteasomes from a *doa4*Δ *pep4* strain (MHY832) that carried a low-copy vector encoding HA-tagged Doa4 [pDOA4-8(HA)]. To help stabilize the 26S complex, 20% glycerol and 2 mM ATP were maintained in all buffers, as has been done for purification of 26S proteasomes from other sources (Kanayama *et al.*, 1992; Ugai *et al.*, 1993). All chromatographic steps were performed on an FPLC system (Pharmacia). A preliminary account of our purification was published previously and used to demonstrate that Sen3 and Cim5 were both components of the yeast 26S proteasome (DeMarini *et al.*, 1995). Table 1 describes a typical purification. Recently, another group developed a related but distinct method for purification of yeast 26S proteasomes (Glickman *et al.*, 1998; Rubin *et al.*, 1998). The purity and activity of the enzymes isolated by the two procedures appear to be quite similar.

After a high-speed centrifugation of crude yeast lysate, the supernatant was chromatographed on a Sephacryl S-400 gel filtration column (Swaffield *et al.*, 1995). As seen in Figure 3A, suc-LLVY-AMC cleaving activity is present in a broad peak centered at ~1600 kDa based on size standards. Little activity is detected at the position of the 20S proteasome (~700 kDa; peak fraction 48, as determined by fractionation of purified 20S proteasomes), suggesting that in yeast most 20S proteasomes are complexed with 19S regulatory particles. Alternatively, 20S proteasome peptidase activity might have been latent; this has been reported for mammalian 20S proteasomes in which low concentrations of SDS can unmask a latent activity (Orlowski, 1990). When 0.01% SDS was added to the assay mixture, a small shoulder of activity was uncovered in fractions eluting after the major 26S peak; however, the size of this activity was still larger than that of the 20S proteasome, suggesting that if it were due to the 20S proteasome, then other proteins were still associated with it (our unpublished results). In addition, anti-20S proteasome immunoblots revealed that most of the 20S subunits were present in fractions corresponding to the peak of suc-LLVY-AMC cleaving activity centered at ~1600 kDa.

HA-Doa4 eluted in a biphasic pattern, with the first peak of protein coinciding with the peak of peptidase activity (26S position, fractions 38–40) and the second peak around a molecular mass of ~700 kDa (fraction 51) (Figure 3B). When the high-speed spin was omitted before S-400 gel filtration, HA-Doa4 was primarily in the 26S proteasome fractions and earlier fractions and not in the second peak, suggesting that a high molecular mass complex(es) that contained HA-Doa4 was broken up during the spin; however, the centrifugation was necessary for obtaining high-purity 26S proteasomes and was therefore retained. Immunoblot analysis using antibodies against the Cim5 subunit of PA700 (Ghislain *et al.*, 1993; DeMarini *et al.*, 1995)

Table 1. Purification of yeast 26S proteasomes

Step	Protein (mg/ml)	Volume (ml)	Total protein (mg)	Total activity (U)[a]	Specific activity (U/mg)	Fold-purified
Crude	12.0	6.0	72	4379	61	
S-400 pool 36–44	0.13	50	6.25	15680	2509	41
Mono-Q pool 33–34	1.23	0.8	0.98	6680	6816	112
Superose 6 pool 32–36	0.08	1.5	0.12	3732	31100	512

[a] One unit is defined as the fluorescence signal of a reaction catalyzed by 1 μl of enzyme in 1 min when suc-LLVY-AMC is in excess (integration time = 1 s).

revealed a Cim5 distribution that coincided with the peptidase activity profile, suggesting that there is little if any free PA700 in yeast cells (our unpublished results). Frequently, a species of HA-Doa4 that migrated more slowly on SDS-PAGE gels could be detected (Figure 3B, fraction 54), but this varied from preparation to preparation. Immunoblotting of crude lysates always revealed this slower migrating band; it may represent a modification, e.g., phosphorylation, of Doa4 that is lost to varying extents during purification. In no case did we detect HA-Doa4 at a position in the gel filtration elution predicted for the monomer (110 kDa, approximately fractions 60–63); however, when HA-Doa4 was overexpressed from a high-copy vector, a small amount of HA-Doa4 protein was found at the position expected for a monomer (see DISCUSSION).

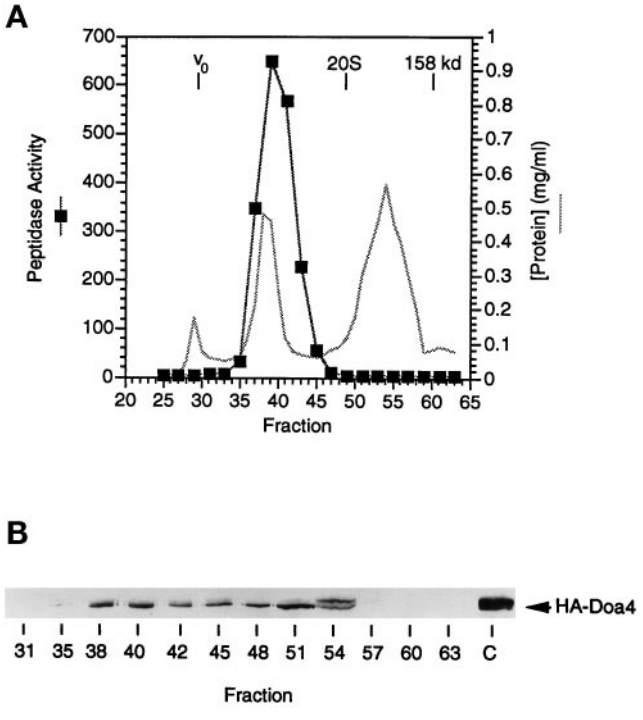

Figure 3. Peptidase activity profile and anti–HA-Doa4 immunoblot analysis of yeast extracts fractionated by Sephacryl S-400 gel filtration. (A) Cleavage of suc-LLVY-AMC in fractions collected from an S-400 column fractionation of extracts from *doa4*Δ cells carrying pDOA4–8(HA). Protein concentration is also plotted. Dextran blue was used to determine the exclusion volume, V_o, and purified 20S proteasomes and aldolase (molecular mass 158 kDa) were used to calibrate the column. (B) Anti-HA immunoblot analysis of HA-Doa4 protein. C, crude lysate.

The S-400 fractions containing the bulk of peptidase activity (fractions 36–44) were pooled. At this stage, a ~40-fold purification of peptidase activity had been achieved (Table 1). Interestingly, a 3.5-fold increase in total activity occurred in this gel filtration step, perhaps because of removal of a proteasome inhibitor. The pooled fractions were applied to a Mono Q anion exchange column, and proteins were eluted with a linear salt gradient. Peptidase activity eluted in a narrow peak (fractions 33 and 34) (Figure 4A). The anion exchange step probably led to some breakdown of the 26S proteasome complex as evidenced by a approximately twofold decline in total activity; however, this effect was compensated by an even greater reduction in total protein (more than sixfold), producing an overall approximately threefold purification over the initial sizing step (Table 1).

Both HA-Doa4, which has a basic pI, and Cim5 coeluted from the Mono Q column in the same fractions as the suc-LLVY-AMC cleaving activity, consistent with an association with the 26S proteasome complex (Figure 4). The salt concentration at the point of elution of the 26S proteasome was estimated to be ~0.6 M. Because the 26S proteasome is known to be labile at this high ionic strength, the buffer was immediately replaced with low ionic strength buffer.

Pooled fractions 33–34 were concentrated and run on a Superose 6 gel filtration column. Proteasomal peptidase activity again eluted at ~1600 kDa (Figure 5A). Both Cim5 and HA-Doa4 eluted in the same fractions as the peptidase activity, and the relative levels of each protein in these fractions closely paralleled the level of peptidase activity (Figure 5B). Proteolysis of polyubiquitinated ^{125}I-lysozyme was measured in the same fractions tested for suc-LLVY-AMC

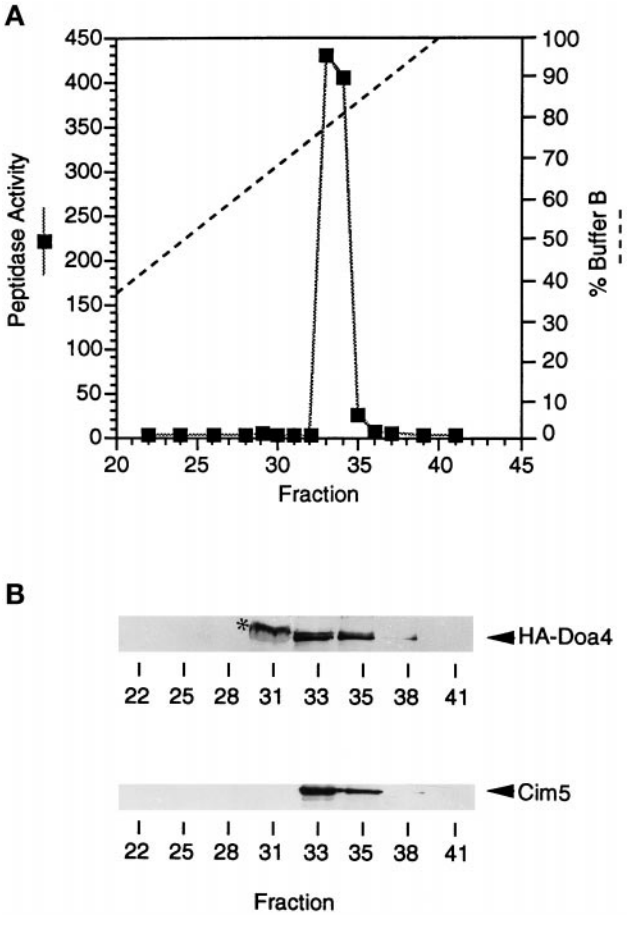

Figure 4. Fractionation of pooled 26S proteasome-containing fractions from a Sephacryl S-400 column by Mono Q anion exchange chromatography. (A) Peptidase activities in fractions collected from a Mono Q HR (5/5) anion exchange column. Elution of proteins was with a linear gradient of 26S buffer containing 0.8 M NaCl (buffer B). (B) Immunoblot analysis of HA-Doa4 and Cim5 proteins in the Mono Q fractions. Asterisk, weak anti-HA cross-reactivity with an abundant yeast protein (not always observed).

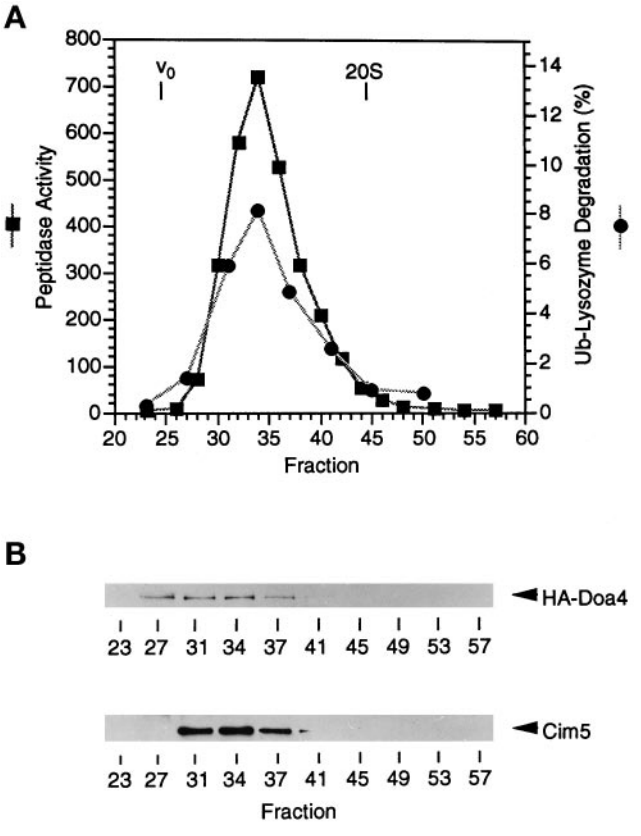

Figure 5. Proteasome fractionation by Superose 6 gel filtration. (A) Peptidase activity and polyubiquitin(Ub)–[^{125}I]-lysozyme degradation in fractions from a Superose 6 gel filtration column. The column was loaded with the pooled and concentrated 26S proteasome-containing Mono Q fractions (Figure 4). Ub–lysozyme degradation is reported as the percentage of total ^{125}I radioactivity that was acid-soluble after a 45 min reaction with 50 μl of each fraction. The elution peak of 20S proteasomes (700 kDa) and the void volume, V_o (5×10^6 D, calibrated with blue dextran) are indicated. (B) Immunoblot analysis of HA-Doa4 and Cim5 proteins in the Superose 6 fractions.

cleavage, and the two activities were found to coelute as well. ^{125}I-lysozyme–conjugate degradation by the yeast protein fractions was fully ATP dependent (Table 2). An ATP regenerating system was required to achieve maximal activity, and degradation in ATP-depleted reactions with the yeast proteasome fractions was identical to a reaction containing only buffer; hence, the ATP-independent degradation that was observed could be traced to the substrate preparation, which had been partially purified from rabbit reticulocyte lysate (Hoffman *et al.*, 1992). SDS-PAGE of the reaction products, followed by autoradiography and densitometric analysis demonstrated that in the ATP-supplemented reaction, polyubiquitinated ^{125}I-lysozyme was consumed without regeneration of free ^{125}I-lysozyme, indicating proteolysis of the substrate rather than deubiquitination (our unpublished results; other substrates for deubiquitination were not assayed).

Superose 6 fractions containing maximal proteasome activity (32–36) were pooled. The specific peptidase activity of this pool was more than 500-fold higher than that of the crude extract (Table 1). Considering that the proteasome is a highly abundant protein, estimated at 0.5–1% of total soluble protein (Orlowski, 1990; Chen and Hochstrasser, 1995), this proteasome preparation would be essentially homogeneous; however, because an apparent inhibitory activity was present before the S-400 gel filtration step (see above), it is difficult to gauge purity by this criterion alone. Nevertheless, both the pattern of subunits visualized on SDS gels and the morphology of particles seen by electron microscopy are very similar to

Table 2. ATP-dependence of ubiquitin–[125I]-lysozyme conjugate degradation by purified yeast 26S proteasomes

Reaction	Enzyme	ATP[a]	% degradation[b]
1	Superose 6 fraction 33	+	19.1
2	Superose 6 fraction 33	−	10.8
3	Buffer	+	10.6

[a] ATP regeneration system (+): 5 mM ATP, 50 mM creatine phosphate, 50 μg/ml creatine kinase; ATP depletion system (−): 25 mM glucose, 25 μg/ml hexokinase.

[b] Average of two independent reactions (45 min).

what has been observed with highly purified 26S proteasomes from other organisms (Figure 6).

SDS-PAGE analysis of the pooled Superose 6 fractions followed by Coomassie Blue staining revealed a complex pattern of protein bands (Figure 6A). A cluster of characteristic 20S subunits was seen along with additional, primarily higher molecular mass species expected for subunits of the 26S proteasome. Electron microscopy (Figure 6B) demonstrated the presence of particles with the characteristic shapes seen previously with 26S proteasomes from other sources (Peters *et al.*, 1991; Yoshimura *et al.*, 1993). These particles appeared to have a PA700 complex attached at each end of the 20S proteasomal cylinder or sometimes at just one end. The mixture of singly and doubly capped 20S proteasomes would explain the slight asymmetry in the activity curve seen in the gel filtration column fractions in Figure 5. Some free 20S particles were also seen in the micrographs (Figure 6B); these may have formed during sample preparation for microscopy. Were this the case, dissociated PA700 regulatory complexes should also have been detected; an additional particle (particle 3), which was probably free PA700, was in fact observed in the samples.

Collectively, these data indicate that a significant percentage of Doa4 protein in yeast cells is associated with active yeast 26S proteasomes. In a later section, we describe additional evidence supporting this inference as well as the idea that proteasome interaction is important for Doa4 function.

Ubp5, a Deubiquitinating Enzyme Related to Doa4

An *S. cerevisiae* ORF first described during the yeast genome sequencing project, YER144c, encodes a protein more highly related to Doa4 than is any other

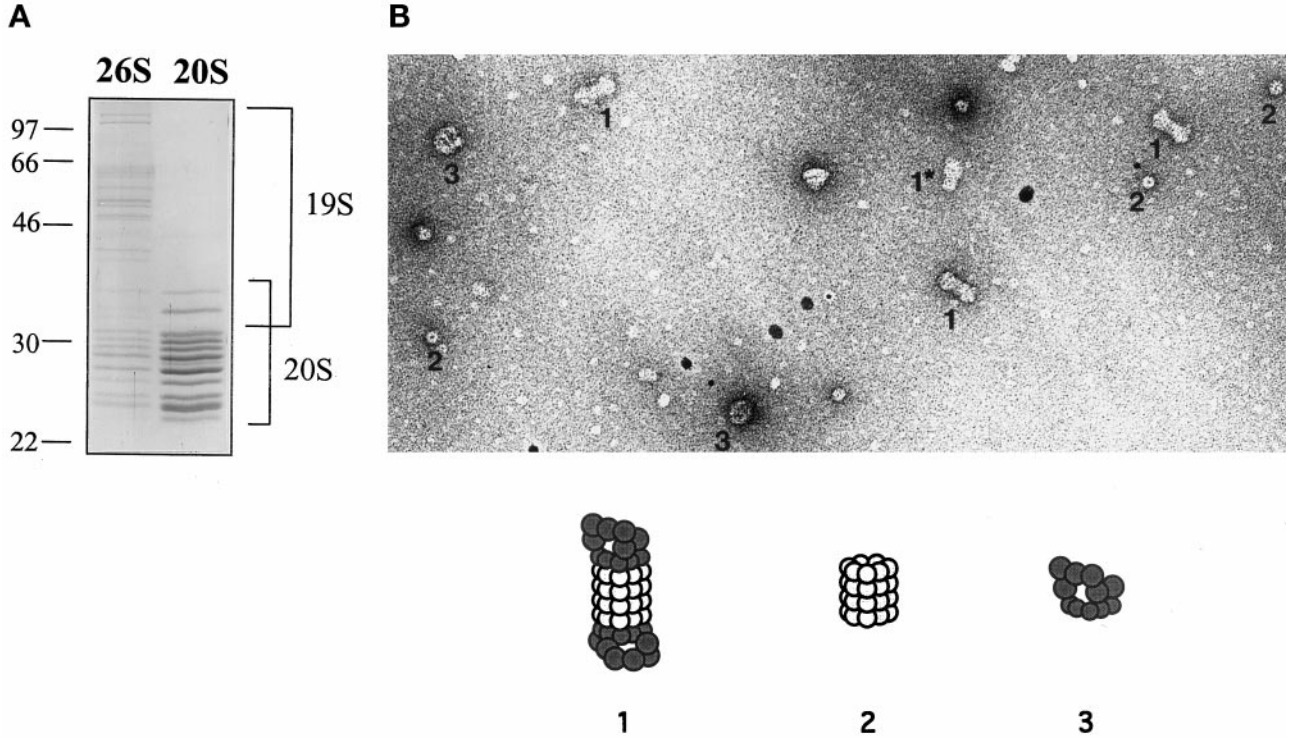

Figure 6. Characterization of purified yeast 26S proteasomes. (A) Analysis of purified 20S and 26S proteasomes by SDS-PAGE followed by Coomassie Blue staining. Protein size standards (in kilodaltons) are indicated. (B) Electron micrograph of purified 26S proteasome complexes negatively stained with uranyl acetate. Several different species are visible: 26S proteasomes with two PA700 complexes attached at either end (1); 20S proteasome with a single PA700 complex (1*); core 20S proteasomes (2); and complexes that are likely to correspond to free PA700 (3).

available protein sequence. The protein, which was named Ubp5 (Xiao *et al.*, 1994), is 44% identical (62% similar) to Doa4 over the entire length of the two ORFs (Figure 7A). In the C-terminal regions of the two proteins beginning at their respective Cys boxes, the degree of similarity is especially high (62% identical; 76% similar). Ubp5 is slightly smaller than Doa4 (805 vs. 926 residues), lacking several peptide segments present in the N-terminal domain of Doa4.

Ubp5 was first tested for deubiquitinating activity. *UBP5* and a reporter gene encoding a ubiquitin–Met–β-galactosidase fusion (Ub-M-βgal) were coexpressed in *E. coli* MC1061 cells (Papa and Hochstrasser, 1993). As measured by anti-βgal immunoblot analysis (Figure 7B, lane 2), approximately half of the Ub-M-βgal was deubiquitinated at steady state in cells expressing Ubp5, indicating that Ubp5 can cleave ubiquitin in peptide linkage with another protein. Using a Lys48-linked diubiquitin molecule as substrate, Ubp5 was also shown to have a ubiquitin isopeptidase activity (Figure 7C). Therefore, like Doa4, Ubp5 is a deubiquitinating enzyme with activity against both peptide and isopeptide-linked ubiquitin moieties.

To create a yeast strain deleted for *UBP5*, one of the two copies in a diploid yeast strain was replaced with the *HIS3* gene by homologous recombination. The deleted sequences (codons 442–716) included the Cys box coding region. When the resulting heterozygotes were sporulated and tetrads were dissected, all four meiotic segregants grew at the same rate in all tetrads, and histidine prototrophy segregated 2:2. The mutant cells exhibited no obvious defects characteristic of mutants in the ubiquitin–proteasome pathway. Mutant *ubp5* cells degraded the test substrates *Deg1*-βgal, L-βgal, and Ub-P-βgal at wild-type rates. Also unlike *doa4*Δ cells, the mutant was neither sensitive to heat shock nor hypersensitive to the arginine analog canavanine, and a *ubp5/ubp5* homozygous diploid sporulated normally. A *doa4*Δ *ubp5*Δ double mutant was constructed to test the possibility that Ubp5 has an overlapping function with Doa4. The *doa4*Δ *ubp5*Δ strain could not be distinguished from a *doa4*Δ single mutant: no further stabilization of *Deg1*-βgal was seen, nor was the double mutant any more sensitive to heat shock or canavanine. Moreover, the ubiquitin conjugate profile of *ubp5*Δ cells could not be distinguished from wild-type cells, whereas the *doa4*Δ *ubp5*Δ double mutant displayed the same characteristic spectrum of ubiquitinated species seen in *doa4*Δ cells. Finally, high-copy expression of *UBP5* in *doa4*Δ cells did not rescue the block to degradation of *Deg1*-βgal (expression of an HA epitope-tagged Ubp5 from a high-copy plasmid led to a large increase in protein level compared with expression of the same derivative from a low-copy vector). We conclude that Ubp5, despite its sequence similarity to Doa4, has little or no overlap in function with Doa4.

An N-Terminal Region of Doa4 Confers Doa4 Function on Ubp5

There are 15 other *UBP* genes in *S. cerevisiae*, yet none of several of these genes that were tested could compensate for loss of *DOA4* even when they were present on high-copy plasmids (F.R. Papa, S. Swaminathan, M. Hochstrasser, unpublished data). This suggested that the Doa4 protein has some unique structural features that impart specificity to its activity in vivo. Given the evidence that Doa4 can associate with proteasomes, one such "specificity element" might be a domain(s) that mediates proteasome binding. We therefore sought to localize a Doa4 specificity determinant(s) using chimeric proteins that fused segments of Doa4 to another Ubp. Ubp5 was chosen for this analysis because segments with similarity to Doa4 are present along the length of the Ubp5 sequence, providing logical positions to place joints in the chimeras that should minimize general structural perturbations.

An initial chimera between *DOA4* and *UBP5* was made by traditional cloning methods to fuse the *DOA4* gene promoter plus coding sequence for the N-terminal region of Doa4 that extended almost to its Cys box (residues 1–560) to a segment of *UBP5* encoding a domain that included the Cys box and extended beyond sequences encoding the Ubp5 C terminus (residues 443–805) (Figure 8A, construct 1). The chimeric gene, when expressed from a YEplac195-based plasmid in a *doa4*Δ strain, provided full Doa4 function as judged by its ability to allow growth of a *doa4*Δ haploid on canavanine-containing medium and to restore normal sporulation to a *doa4*Δ*/doa4*Δ diploid. In the same cells, *Deg1*-βgal levels, as measured by activity assays, were reduced to an amount ~30% higher than that seen in wild-type cells, suggesting that the protein encoded by the chimeric gene provided substantial albeit not quite wild-type Doa4 function (Figure 9A).

Six additional Doa4-Ubp5 chimeras were constructed (Figure 8A). Because of the lack of convenient restriction sites in *DOA4* and *UBP5*, we devised a convenient method for constructing gene fusions. This method, which we call PCR–GR, has general utility and is described in detail in MATERIALS AND METHODS (Figure 1). PCR–GR was performed in strain MHY905, a *doa4*Δ mutant that carried an integrated *Deg1-lacZ* reporter gene. We recovered the recombinant plasmids and transformed them back into MHY905 cells to confirm that any changes in phenotype were due to the plasmid and not to chromosomal mutations. The plasmids were also transformed into bacteria that expressed a Ub-L-βgal reporter; all recombinant proteins had deubiquitinating activity against this substrate. The *UBP5* gene used in the gap repair constructions had a sequence encoding a triple-HA tag at the 3′ end of the ORF, allowing us to check protein levels of the chimeric enzymes. All chi-

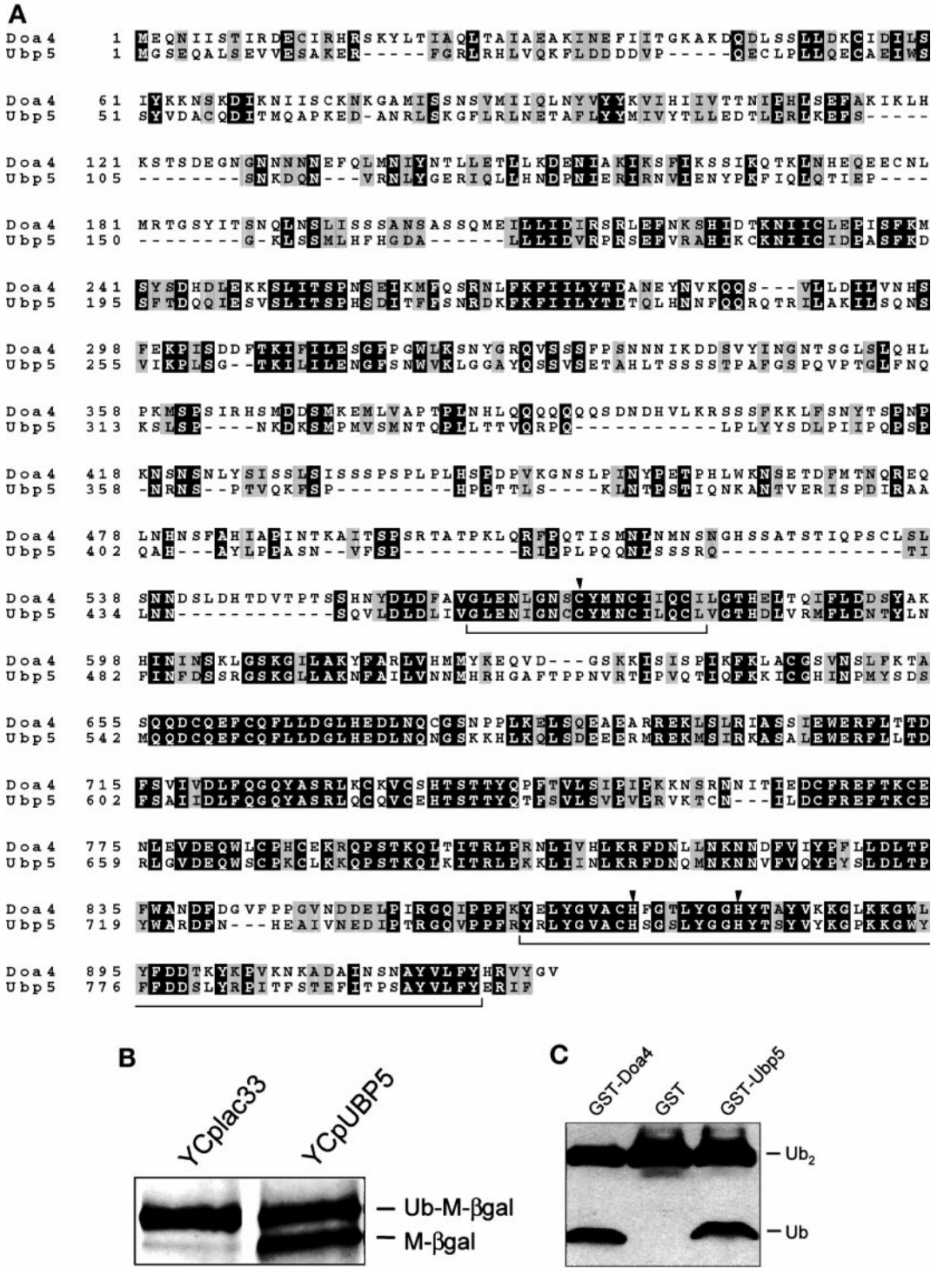

Figure 7. An enzyme closely related to Doa4 encoded by the yeast *UBP5* (YER144c) gene. (A) Sequence alignment of Doa4 and Ubp5. The two proteins were aligned with the ClustalW algorithm followed by manual adjustment. Identical residues are boxed in black, and structurally related residues are boxed in gray. The Cys and His boxes are indicated by brackets, and the conserved Cys and His residues in these two motifs are marked by arrowheads. (B) Cleavage of a ubiquitin–protein fusion by Ubp5. Shown is an anti-βgal Western immunoblot analysis of extracts from MC1061 cells harboring a plasmid expressing Ub-M-βgal and either YCplac33 vector or YCplac33-UBP5. (C) Ubiquitin isopeptidase activity of Ubp5 using a Lys48-linked diubiquitin substrate. Substrate was incubated at 30°C in *E. coli* extracts expressing either GST or GST-Ubp5. Partially purified GST-Doa4 was used as a control.

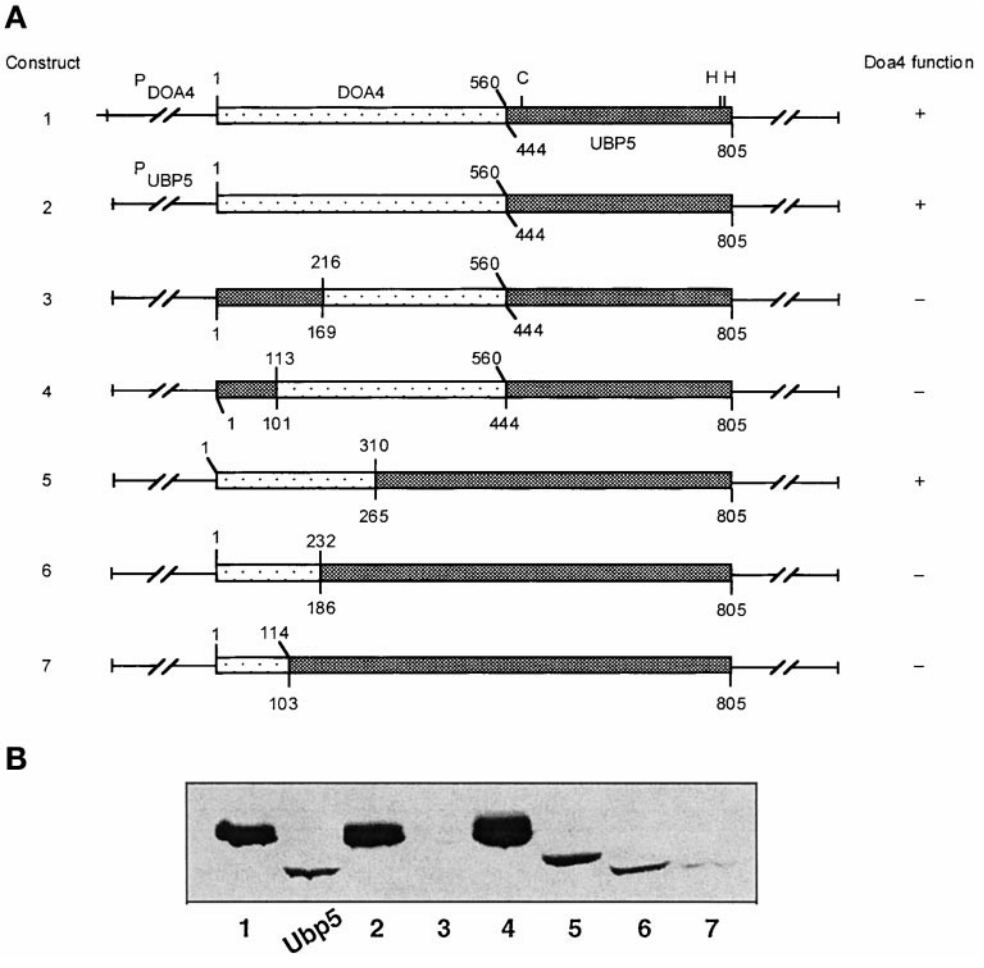

Figure 8. Expression of chimeric Doa4-Ubp5 proteins in *doa4*Δ cells. (A) Schematics of chimeric *DOA4-UBP5* genes specifying the sites of fusion. Lightly stippled boxes correspond to *DOA4* coding sequences, and darkly stippled boxes correspond to those of *UBP5*. Doa4 function was assayed by growth of *doa4*Δ haploid cells on 0.8 μg/ml canavanine and by sporulation of *doa4*Δ/*doa4*Δ diploid cells. (B) Anti-HA immunoblot analysis of extracts from *doa4*Δ cells expressing the chimeras diagrammed in A and from cells expressing Ubp5-HA (lane marked Ubp5).

meras were expressed in yeast except construct 3, which was undetectable by immunoblot analysis (Figure 8B).

The chimeras were tested for their ability to restore growth of *doa4*Δ mutant cells on canavanine; in addition, the ability of the chimeras to support sporulation of a *doa4*Δ/*doa4*Δ diploid was tested. By both tests, constructs 1, 2, and 5 were fully active (Figure 8A). In addition, steady-state *Deg1*-βgal levels were measured by quantitative βgal activity assays (Figure 9A). Constructs 1, 2, and 5 all caused a reduction of *Deg1*-βgal levels relative to that seen in *doa4*Δ cells. In contrast, neither a high-copy *UBP5* plasmid nor plasmids encoding Doa4-Ubp5 chimeras 3, 4, 6, or 7 had *doa4*Δ-complementing activity by any of the above assays. Finally, we examined extracts from all of these cells by antiubiquitin immunoblot analysis (Figure 9B). Mutant *doa4*Δ cells that harbored constructs with *doa4*Δ-complementing activity, but not those with non-complementing plasmids, contained greatly reduced levels of the small (poly)ubiquitinated species seen in *doa4*Δ cells. The levels were still slightly above those observed in wild-type cells, again indicating that Doa4 function was not quite completely restored. As is evident in Figure 9, levels of the apparent ubiquitin–peptide conjugates correlated very closely with steady-state levels of the *Deg1*-βgal reporter (and therefore should correlate inversely with rates of *Deg1*-βgal degradation).

The complementing *DOA4-UBP5* construct with the shortest *DOA4* sequence was chimera 5, in which the only *DOA4*-derived sequences are those encoding the N-terminal 310 residues of Doa4. All of the signature sequences that are thought to define the catalytic domain of the Ubp enzyme family in this chimera were derived from Ubp5. The Doa4-Ubp5 chimera with the next smallest N-terminal Doa4 segment (#6, Doa4 residues 1–232) lacked Doa4 activity in vivo, as did construct 4, with Doa4 residues 113–310. Therefore, the N-terminal 310 residues of Doa4 were sufficient for imparting Doa4 function to the heterologous Ubp5 catalytic domain, and Doa4 residues 233–310 and 1–112 were necessary in this context. The N-terminal 310 residues of Doa4 also appeared to be necessary for

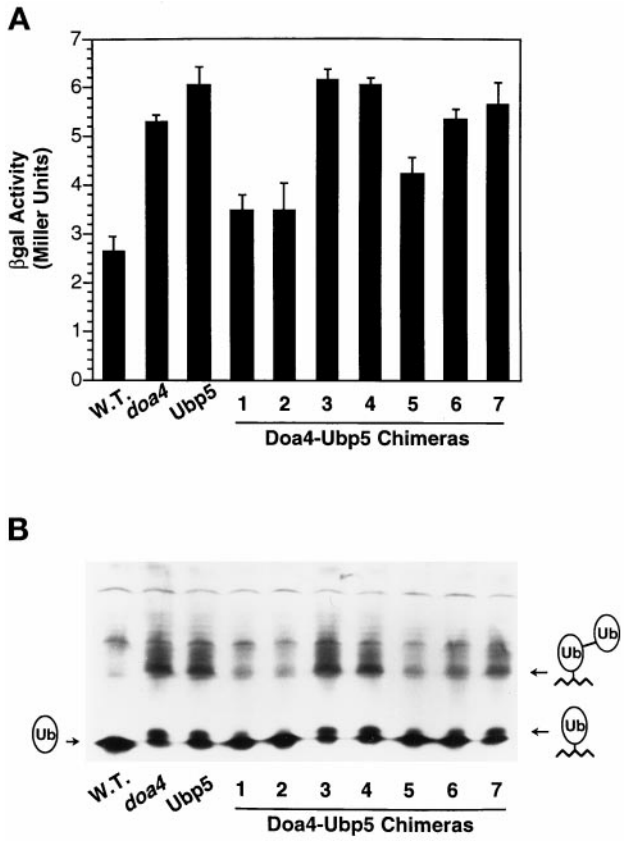

Figure 9. Close correlation between *Deg1-*βgal accumulation and levels of low molecular mass (poly)ubiquitin conjugates in *doa4*Δ cells expressing Doa4-Ubp5 chimeras. (A) βgal activity assays of extracts made from yeast cells with an integrated *Deg1-lacZ* reporter gene. W.T., wild-type strain (MHY501). The remaining strains harbor a chromosomal deletion of *DOA4* and carry the empty YEplac195 vector (*doa4*) or plasmids expressing Ubp5 or the Doa4-Ubp5 chimeras. Numbering of chimeras as in Figure 8. (B) Antiubiquitin immunoblot analysis of same strains as in A.

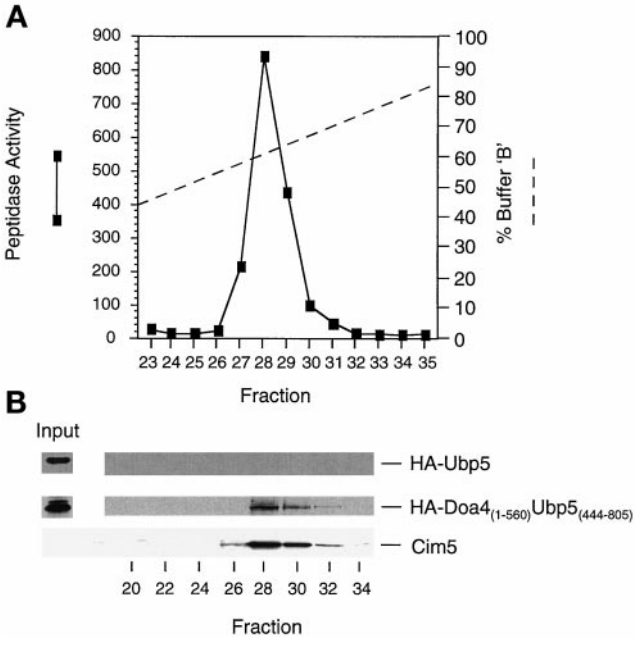

Figure 10. Cofractionation of a Doa4-Ubp5 chimera with 26S proteasomes. Top, suc-LLVY-AMC–cleaving activity of Mono Q column fractions. Pooled 26S proteasome-containing fractions from an S-400 gel filtration provided the input. Lysate was made from *doa4*Δ cells expressing the HA-tagged $Doa4_{1-560}$–$Ubp5_{444-805}$ chimera from a YEplac195-based plasmid. Bottom, Immunoblot detection of HA-Doa4-Ubp5, HA-Ubp5, and Cim5 proteins. At left are shown anti-HA immunoblots of HA-tagged proteins in the pooled S-400 fractions that provided the inputs to the Mono Q column.

in vivo activity in the context of the intact Doa4 protein because a Doa4 variant lacking these residues failed to complement a *doa4*Δ mutant (our unpublished results).

A Doa4-Ubp5 Chimera Can Associate with the 26S Proteasome

One hypothesis for the function of the specificity element(s) contained in the N-terminal domain of Doa4 is that it participates in Doa4 binding to the 26S proteasome. To test this idea, we determined whether a *doa4*Δ-complementing Doa4-Ubp5 chimera could also associate with proteasomes (Figure 10). We chose $Doa4_{1-560}$–$Ubp5_{444-805}$ (chimera 2) for this analysis because levels of this chimera were slightly higher than those of $Doa4_{1-310}$–$Ubp5_{265-805}$, and the *doa4*Δ-complementing capabilities of these two constructs did not differ significantly. After a high speed centrifugation, extracts from *doa4*Δ cells expressing either the HA–Doa4-Ubp5 chimera or HA–Ubp5 were fractionated by S-400 gel filtration. Ubp5 eluted over a broad range of fractions, including some of the proteasome-containing fractions, (Figure 10, Input), so this chromatographic step was insufficient to distinguish Ubp5 from the Doa4-Ubp5 chimera. Therefore, the peak proteasome fractions from each run were pooled and chromatographed on a Mono Q column (Figure 10). As had been found with full-length Doa4, the functional Doa4-Ubp5 chimera cofractionated precisely with the 26S proteasome-containing fractions, the latter followed by means of peptidase activity assays and anti-Cim5 immunoblot analysis. In contrast, Ubp5 appeared not to bind the anion exchange matrix under the conditions used and was undetectable in the proteasome-containing fractions. The correlation between *doa4*Δ-complementing activity and ability to cofractionate with the proteasome demonstrated by these data suggests that physical association of Doa4 with the protease is physiologically relevant.

DISCUSSION

In the present work, we have described a combination of biochemical and genetic results indicating that the Doa4 deubiquitinating enzyme can associate with the yeast 26S proteasome and that the ability of Doa4 to associate with the proteasome correlates with Doa4 functional competence in vivo. As discussed below, these results shed light on the mechanism of Doa4 action in vivo and on its pivotal but complex role in the yeast ubiquitin system.

Doa4 Association with the 26S Proteasome

As noted in the INTRODUCTION, several lines of evidence had initially suggested that Doa4 and proteasome action might be linked (Papa and Hochstrasser, 1993). On the basis of these considerations, we hypothesized that the Doa4 enzyme deubiquitinated proteolytic intermediates associated with the 26S proteasome, allowing efficient reutilization of both ubiquitin and proteasomes (Papa and Hochstrasser, 1993). The experiments described here were designed to test key elements of this model. Our main approach was to isolate highly purified 26S proteasomes and determine whether any of the cellular Doa4 protein cofractionated with the protease.

When this work was initiated, no suitable purification was available for the yeast 26S proteasome, so we developed the procedure described in RESULTS. Although it is difficult to determine the purity of a large complex composed of more than 30 distinct polypeptides, estimates based on the fold-purification of specific peptidase activity suggest that 26S proteasomes were purified to >95% purity by weight. The yeast enzyme isolated in this way is very similar to 26S proteasomes from other organisms in terms of subunit pattern, size, particle morphology, ability to degrade polyubiquitinated substrate, and ATP dependence. Furthermore, this purification was used previously to demonstrate that Cim5 and Sen3 are components of the yeast 26S proteasome (DeMarini *et al.*, 1995), consistent with the finding that orthologues of these proteins are subunits of mammalian PA700 particles (DeMartino *et al.*, 1994; Yokota *et al.*, 1996).

A fully functional, HA-tagged version of Doa4, expressed from a low-copy vector to avoid overexpression artifacts, cofractionates with 26S proteasomes throughout the purification, which includes a high-speed centrifugation and three distinct FPLC fractionation steps. On the other hand, SDS-PAGE/silver-stain analysis of proteasomes purified from wild-type and *doa4*Δ cells did not reveal the loss of a band of the size expected for HA-Doa4. There are several possible explanations for this observation. HA-Doa4 might be present in substoichiometric amounts, it might be concealed by a similar-sized polypeptide (e.g., Nas1/Hrd2), and/or it might stain poorly with silver. Another explanation is that the interaction between Doa4 and the proteasome is weak, and much of Doa4 is lost during purification. We have seen that Doa4 is not limited entirely to the 26S proteasome fractions in the first gel filtration step. It elutes in two broad peaks in roughly equal amounts, the larger complex coinciding with the peak of 26S proteasomes; however, this 26S proteasome-coincident fraction of HA-Doa4 continues to cofractionate almost completely with the 26S proteasome in subsequent steps, suggesting that under our purification conditions (low salt, high glycerol, and ATP), association of Doa4 and the 26S proteasome is quite stable. When physiological levels of Doa4 were expressed, no Doa4 was seen in the S-400 column fractions that would have contained monomeric protein.

We have also purified 26S proteasomes from cells overproducing HA-Doa4 (our unpublished results). Under these conditions, some apparently monomeric Doa4 is seen in the S-400 gel filtration step; however, in the subsequent Mono Q and Superose 6 fractionations, approximately three- to fourfold more Doa4 (relative to the amount seen with physiological levels of *DOA4* expression) eluted in the 26S proteasome fractions and was not detected in any other assayed fractions. These results suggest that not all proteasomes have bound Doa4 when Doa4 is expressed at normal levels in exponentially growing cells, but enhanced expression of Doa4 allows proteasome binding sites to be saturated. We previously reported that Doa4 levels are partially rate-limiting for degradation of several substrates in vivo (Papa and Hochstrasser, 1993). An idea consistent with all the available data is that the Doa4–proteasome interaction is dynamic, with Doa4 cycling between 26S proteasome complexes in vivo to cleave ubiquitin from polyubiquitinated proteolytic intermediates. Because such reactions should engender significant changes in rates of substrate degradation, regulation of Doa4-catalyzed deubiquitination may contribute significantly to the control of proteasome-mediated proteolysis in the cell (Hochstrasser, 1995). Regulation may occur through modification of Doa4 (Figure 3B), changes in Doa4 expression, or modulation of its association/dissociation from the proteasome.

As noted earlier, an alternative protocol for purification of yeast 26S proteasomes has recently been described (Glickman *et al.*, 1998; Rubin *et al.*, 1998). By the same criteria used to evaluate our preparations (see above), proteasomes purified by this alternative procedure also appear to be very similar to 26S particles from other species. Peptide sequence information from subunits of the purified proteasome led to the identification of 17 subunits of the 19S regulatory particle, all but one of which had been found previously in proteasomes from yeast and other organisms (see Glickman *et al.* [1998] and references therein). Doa4 was not among the identified subunits. This is not altogether surprising in light of the data presented here, which indicate that Doa4 is not likely to be present in stoichiometric amounts in proteasomes at normal *DOA4* expression levels. One or more of the

differences in the two purification schemes could also account for the failure by Glickman *et al.* (1998) to detect Doa4. The same group also did not identify Son1, another protein recently shown to be a subunit of the yeast 26S proteasome (Fujimuro *et al.*, 1998). There are additional examples of proteins from both yeast and mammals for which there is evidence for association with proteasomes but which were not identified by systematic subunit analyses of purified 26S proteasomes (Dai *et al.*, 1998; Schauber *et al.*, 1998).

Such results obviously raise the question of whether a protein such as Doa4 that copurifies with the proteasome is merely a contaminant in the proteasome preparations. The extremely similar fractionation profiles of Doa4, Cim5, 20S proteasome subunits, and proteasome activity on several different columns argue strongly against a chance overlap of Doa4-containing complexes and 26S proteasomes. Furthermore, we have shown that the Ubp5 enzyme, which cannot replace Doa4 functionally in the cell and shows no evidence of proteasome association, acquires strong *doa4*Δ-complementing activity when its N-terminal ~300 residues are replaced with the corresponding region of Doa4, and the hybrid protein copurifies with 26S proteasomes. Although the Doa4-Ubp5 chimera data are correlative, they suggest that the Doa4–proteasome interaction is functionally significant. This last inference is underscored by the genetic interaction between mutations in *DOA4* and proteasome genes, as reported here, and the earlier molecular genetic data arguing for Doa4 involvement late in the ubiquitin–proteasome pathway.

Mechanism of Doa4 Action In Vivo

Purified rabbit 26S proteasomes appear to possess an ATP-dependent ubiquitin isopeptidase activity (Eytan *et al.*, 1993), and a bovine ubiquitin isopeptidase activity independent of ATP was found to be tightly associated with PA700 (Lam *et al.*, 1997). The latter activity has the intriguing feature of being able to "trim" ubiquitin monomers from the distal end of polyubiquitinated proteins. This activity may allow substrates to be released from proteasomes without degradation, or it could enhance degradation by facilitating release of the polyubiquitinated substrate from its initial proteasome binding site for translocation to the catalytic core. Recent evidence strongly suggests that the PA700 isopeptidase is a member of the ubiquitin C-terminal hydrolase (UCH) family rather than being a UBP (R. Cohen, personal communication). *S. cerevisiae* has only one UCH enzyme, Yuh1, and this enzyme is almost certainly not a component of the proteasome (Liu *et al.*, 1989; Glickman *et al.*, 1998). We detect a relatively weak deubiquitinating activity in our 26S proteasome preparations but have not yet determined whether this derives from Doa4 (our unpublished data).

How is Doa4 deubiquitinating activity coupled to proteasome action? In our original model, we suggested that Doa4 cleaves ubiquitin from (poly)ubiquitinated peptide remnants generated by the proteasome and that this activity is necessary for proteasome and ubiquitin recycling (Papa and Hochstrasser, 1993). The substantial reduction in levels of the small (poly)ubiquitinated species in *doa4*Δ cells that occurs with introduction of the *doa3-1* proteasomal mutation is consistent with the idea that the proteasome helps generate these species; however, it is difficult to determine whether these ubiquitin conjugates are normal proteolytic intermediates in wild-type yeast because they are very difficult to detect in these cells. Hence, it remains plausible that Doa4 can act on proteasome-bound polyubiquitinated proteins before the initiation of substrate cleavage, at least with some substrates. The timing of Doa4 action relative to that of other events in the 26S proteasome degradation mechanism remains a central issue for future work.

Finally, it is worth emphasizing that the *doa4* mutant phenotype is complex, and Doa4 activity may not necessarily be limited to proteasome-bound substrates. The presence of a significant population of Doa4 molecules that is not tightly associated with 26S proteasomes is consistent with this idea (Figure 3). Ubiquitin levels are often reduced in *doa4*Δ cells, and this can result in defects in ubiquitin-dependent but proteasome-independent pathways (S. Swaminathan, M. Hochstrasser, unpublished observations). Further biochemical and genetic studies should clarify when Doa4 action can be mechanistically uncoupled from that of the proteasome (Singer *et al.*, 1996; Galan and Haguenauer-Tsapis, 1997; Loayza and Michaelis, 1998).

Architecture of UBP-Class Deubiquitinating Enzymes

The current work includes the first extensive structure–function study of any DUB enzyme beyond mutation of putative active site residues. Doa4-Ubp5 domain swap experiments suggest that UBPs have a modular architecture, with a catalytic "domain," defined as the sequence extending from the Cys box to the His box, as well as one or more separable specificity determinants. This is likely to be an oversimplified picture of UBP functional architecture. For instance, many UBPs have additional sequences of varied length and composition within the catalytic domain (as defined above), and these elements are likely to contribute to the specialization of UBPs as well. Nevertheless, the regions of greatest variability in both length and sequence among these enzymes are the segments N-terminal to the Cys boxes. For example, the only yeast proteins with any obvious similarity to this region of Doa4 are Ubp5 and, much more distantly, Ubp7. The N-terminal domains of UBPs

therefore have the greatest potential for conferring functional specialization, and the Doa4-Ubp5 chimeras provide the first evidence in support of this conjecture. We recently isolated a functional homolog of Doa4 from *Kluveromyces lactis* (A. Amerik, M. Hochstrasser, unpublished data). The region of highest similarity between the two orthologues in their N-terminal domains encompasses residues 14–324 of *S. cerevisiae* Doa4. The extent of this alignment is remarkably similar to the minimal specificity domain defined with the Doa4-Ubp5 chimeras (Figure 8).

Mammalian functional homologs of Doa4 have not yet been identified. One of the proteins in the current sequence databases with the highest similarity to Doa4 is human UBPY (Naviglio *et al.*, 1998). Interestingly, this enzyme, like Doa4, appears to have a global role in regulating the cellular ubiquitin system: microinjection of antisense sequences both inhibited cell proliferation and led to an accumulation of apparent polyubiquitin–protein conjugates. Analogous to Doa4, UBPY protein also appears as a doublet by immunoblot analysis and may be a phosphoprotein (Naviglio *et al.*, 1998). It remains to be seen whether the human *UBPY* gene is in fact a *DOA4* orthologue.

It is generally assumed that deubiquitinating enzymes have unique specificities that restrict their activity to distinct cellular substrates. Such enzymatic specificity has been clearly shown for isopeptidase T/Ubp14 (Wilkinson *et al.*, 1995; Amerik *et al.*, 1997). Alternatively, or in addition, DUB action may be restricted by differential localization within the cell. The evidence that Doa4 binds to the 26S proteasome and that this is likely to be functionally relevant implies that at least part of the in vivo specificity of this enzyme lies in its differential compartmentalization. Further biochemical studies will be necessary to determine whether Doa4 shows strong preferences toward particular ubiquitinated substrates and whether this specificity is altered by its association with the proteasome.

ACKNOWLEDGMENTS

We thank Q. Deveraux and M. Rechsteiner for radiolabeled ubiquitin–lysozyme conjugates, K. Tanaka for antibodies to yeast Cim5 and 20S proteasomes, C. Pickart for antibody to ubiquitin, R. Josephs for electron microscopy of proteasomes, J. Swaffield and G. DeMartino for suggesting conditions for cell lysis and the initial S-400 fractionation, Casey Arendt for purified 20S proteasomes, and R. Rylaarsdam and S. Swaminathan for comments on this manuscript. This work was supported by National Institutes of Health grant GM53756 to M.H.

REFERENCES

Akopian, T.N., Kisselev, A.F., and Goldberg, A.L. (1997). Processive degradation of proteins and other catalytic properties of the proteasome from *Thermoplasma acidophilum*. J. Biol. Chem. *272*, 1791–1798.

Amerik, A.Y., Swaminathan, S., Krantz, B.A., Wilkinson, K.D., and Hochstrasser, M. (1997). In vivo disassembly of free polyubiquitin chains by yeast Ubp14 modulates rates of protein degradation by the proteasome. EMBO J. *16*, 4826–4838.

Ausubel, F.M., Brent, R., Kingston, R.E., Moore, D.D., Seidman, J.G., Smith, J.A., and Struhl, K. (1989). Current Protocols in Molecular Biology, New York: John Wiley & Sons.

Baker, R.T., Tobias, J.W., and Varshavsky, A. (1992). Ubiquitin-specific proteases of *Saccharomyces cerevisiae*. Cloning of UBP2 and UBP3, and functional analysis of the UBP gene family. J. Biol. Chem. *267*, 23364–23375.

Baudin, A., Ozier-Kalogeropoulos, O., Denouel, A., Lacroute, F., and Cullin, C. (1993). A simple and efficient method for direct gene deletion in *Saccharomyces cerevisiae*. Nucleic Acids Res. *21*, 3329–3330.

Baumeister, W., Walz, J., Zuhl, F., and Seemuller, E. (1998). The proteasome: paradigm of a self-compartmentalizing protease. Cell *92*, 367–380.

Chen, P., and Hochstrasser, M. (1995). Biogenesis, structure, and function of the yeast 20S proteasome. EMBO J. *14*, 2620–2630.

Chen, P., Johnson, P., Sommer, T., Jentsch, S., and Hochstrasser, M. (1993). Multiple ubiquitin-conjugating enzymes participate in the in vivo degradation of the yeast MATα2 repressor. Cell *74*, 357–369.

Coux, O., Tanaka, K., and Goldberg, A.L. (1996). Structure and functions of the 20S and 26S proteasomes. Annu. Rev. Biochem. *65*, 801–847.

Dai, R.M., Chen, E., Longo, D.L., Gorbea, C.M., and Li, C.C. (1998). Involvement of valosin-containing protein, an ATPase copurified with IκBα and 26 S proteasome, in ubiquitin-proteasome-mediated degradation of IκBα. J. Biol. Chem. *273*, 3562–3573.

DeMarini, D.J., Papa, F.R., Swaminathan, S., Ursic, D., Rasmussen, T.P., Culbertson, M.R., and Hochstrasser, M. (1995). The yeast SEN3 gene encodes a regulatory subunit of the 26S proteasome complex required for ubiquitin-dependent protein degradation in vivo. Mol. Cell. Biol. *15*, 6311–6321.

DeMartino, G.N., Moomaw, C.R., Zagnitko, O.P., Proske, R.J., Ma, C.-P., Afendis, S.J., Swaffield, J.C., and Slaughter, C.A. (1994). PA700, an ATP-dependent activator of the 20S proteasome, is an ATPase containing multiple members of a nucleotide-binding protein family. J. Biol. Chem. *269*, 20878–20884.

Eytan, E., Armon, T., Heller, H., Beck, S., and Hershko, A. (1993). Ubiquitin C-terminal hydrolase activity associated with the 26S protease complex. J. Biol. Chem. *268*, 4668–4674.

Falquet, L., Paquet, N., Frutiger, S., Hughes, G.J., Hoang-Van, K., and Jaton, J.C. (1995). A human deubiquitinating enzyme with both isopeptidase and peptidase activities in vitro. FEBS Lett. *359*, 73–77.

Fischer, M., Hilt, W., Richter-Ruoff, B., Gonenm, H., Ciechanover, A., and Wolf, D.H. (1994). The 26S proteasome of the yeast *Saccharomyces cerevisiae*. FEBS Lett. *355*, 69–75.

Flaman, J.M., *et al.* (1995). A simple p53 functional assay for screening cell lines, blood, and tumors. Proc. Natl. Acad. Sci. USA *92*, 3963–3967.

Fujimuro, M., Tanaka, K., Yokosawa, H., and Toh-e, A. (1998). Son1p is a component of the 26S proteasome of the yeast *Saccharomyces cerevisiae*. FEBS Lett. *423*, 149–154.

Galan, J., and Haguenauer-Tsapis, R. (1997). Ubiquitin Lys63 is involved in ubiquitination of a yeast plasma membrane protein. EMBO J. *16*, 5847–5854.

Ghislain, M., Udvardy, A., and Mann, C. (1993). *S. cerevisiae* 26S protease mutants arrest cell division in G2/metaphase. Nature *366*, 358–362.

Gietz, R.D., and Sugino, A. (1988). New yeast-*Escherichia coli* shuttle vectors constructed with in vitro mutagenized yeast genes lacking six-bp restriction sites. Gene *74*, 527–534.

Glickman, M.H., Rubin, D.M., Fried, V.A., and Finley, D. (1998). The regulatory particle of the *Saccharomyces cerevisiae* proteasome. Mol. Cell. Biol. *18*, 3149–3162.

Hilt, W., and Wolf, D.H. (1996). Proteasomes: destruction as a program. Trends Biochem. Sci. *21*, 96–102.

Hochstrasser, M. (1995). Ubiquitin, proteasomes, and the regulation of intracellular protein degradation. Curr. Opin. Cell Biol. *7*, 215–223.

Hochstrasser, M. (1996). Ubiquitin-dependent protein degradation. Annu. Rev. Genet. *30*, 405–439.

Hochstrasser, M., Papa, F.R., Chen, P., Swaminathan, S., Johnson, P., Stillman, L., Amerik, A., and Li, S.-J. (1995). The DOA pathway: studies on the functions and mechanisms of ubiquitin-dependent protein degradation in the yeast *Saccharomyces cerevisiae*. Cold Spring Harbor Symp. Quant. Biol. *60*, 503–513.

Hochstrasser, M., and Varshavsky, A. (1990). In vivo degradation of a transcriptional regulator: the yeast α2 repressor. Cell *61*, 697–708.

Hoffman, L., Pratt, G., and Rechsteiner, M. (1992). Multiple forms of the 20 S multicatalytic and the 26 S ubiquitin/ATP-dependent proteases from rabbit reticulocyte lysate. J. Biol. Chem. *267*, 22362–22368.

Kanayama, H.O., Tamura, T., Ugai, S., Kagawa, S., Tanahashi, N., Yoshimura, T., Tanaka, K., and Ichihara, A. (1992). Demonstration that a human 26S proteolytic complex consists of a proteasome and multiple associated protein components and hydrolyzes ATP and ubiquitin-ligated proteins by closely linked mechanisms. Eur. J. Biochem. *206*, 567–578.

Lam, Y.A., Xu, W., DeMartino, G.N., and Cohen, R.E. (1997). Editing of ubiquitin conjugates by an isopeptidase in the 26S proteasome. Nature *385*, 737–740.

Liu, C.C., Miller, H.I., Kohr, W.J., and Silber, J.I. (1989). Purification of a ubiquitin protein peptidase from yeast with efficient in vitro assays. J. Biol. Chem. *264*, 20331–20338.

Loayza, D., and Michaelis, S. (1998). Role for the ubiquitin-proteasome system in the vacuolar degradation of Ste6p, the a-factor transporter in *Saccharomyces cerevisiae*. Mol. Cell. Biol. *18*, 779–789.

Ma, C.P., Vu, J.H., Proske, R.J., Slaughter, C.A., and DeMartino, G.N. (1994). Identification, purification, and characterization of a high molecular weight, ATP-dependent activator (PA700) of the 20 S proteasome. J. Biol. Chem. *269*, 3539–3547.

Ma, H., Kunes, S., Schatz, P., and Botstein, D. (1987). Plasmid construction by homologous recombination in yeast. Gene *58*, 201–216.

Muhlrad, D., Hunter, R., Parker, R. (1992). A rapid method for localized mutagenesis of yeast genes. Yeast *8*, 79–82.

Naviglio, S., Mattecucci, C., Matoskova, B., Nagase, T., Nomura, N., Di Fiore, P.P., and Draetta, G.F. (1998). UBPY: a growth-regulated human ubiquitin isopeptidase. EMBO J. *17*, 3241–3250.

Orlowski, M. (1990). The multicatalytic proteinase complex, a major extralysomal proteolytic system. Biochemistry *29*, 10289–10297.

Papa, F., and Hochstrasser, M. (1993). The yeast *DOA4* gene encodes a deubiquitinating enzyme related to a product of the human *tre-2* oncogene. Nature *366*, 313–319.

Peters, J.M., Harris, J.R., and Kleinschmidt, J.A. (1991). Ultrastructure of the approximately 26S complex containing the approximately 20S cylinder particle (multicatalytic proteinase/proteasome). Eur. J. Cell. Biol. *56*, 422–432.

Pickart, C.M. (1997). Targeting of substrates to the 26S proteasome. FASEB J. *11*, 1055–1066.

Rubin, D.M., Glickman, M.H., Larsen, C.N., Dhruvakumar, S., and Finley, D. (1998). Active site mutants in the six regulatory particle ATPases reveal multiple roles for ATP in the proteasome. EMBO J. *17*, 4909–4919.

Schauber, C., Chen, L., Tongaonkar, P., Vega, I., Lambertson, D., Potts, W., and Madura, K. (1998). Rad23 links DNA repair to the ubiquitin/proteasome pathway. Nature *391*, 715–718.

Singer, J.D., Manning, B.M., and Formosa, T. (1996). Coordinating DNA replication to produce one copy of the genome requires genes that act in ubiquitin metabolism. Mol. Cell. Biol. *16*, 1356–1366.

Swaffield, J.C., Melcher, K., and Johnston, S.A. (1995). A highly conserved ATPase protein as a mediator between acidic activation domains and the TATA-binding protein. Nature *374*, 88–91.

Tyers, M., Tokiwa, G., Nash, R., and Futcher, B. (1992). The Cln3-Cdc28 kinase complex of *S. cerevisiae* is regulated by proteolysis and phosphorylation. EMBO J. *11*, 1773–1784.

Udvardy, A. (1993). Purification and characterization of a multiprotein component of the *Drosophila* 26 S (1500 kDa) proteolytic complex. J. Biol. Chem. *268*, 9055–9062.

Ugai, S., Tamura, T., Tanahashi, N., Takai, S., Komi, N., Chung, C.H., Tanaka, K., and Ichihara, A. (1993). Purification and characterization of the 26S proteasome complex catalyzing ATP-dependent breakdown of ubiquitin-ligated proteins from rat liver. J. Biochem. *113*, 754–768.

Varshavsky, A. (1997). The ubiquitin system. Trends Biochem. Sci. *22*, 383–387.

Wilkinson, K.D. (1995). Roles of ubiquitinylation in proteolysis and cellular regulation. Annu. Rev. Nutr. *15*, 161–189.

Wilkinson, K.D., and Hochstrasser, M. (1998). Deubiquitinating enzymes. In: Ubiquitin and the Biology of the Cell, ed. J.M. Peters, J.R. Harris, and D. Finley, New York: Plenum Press, 99–125.

Wilkinson, K.D., Tashayev, V.L., O'Connor, L.B., Larsen, C.N., Kasperek, E., and Pickart, C.M. (1995). Metabolism of the polyubiquitin degradation signal: structure, mechanism, and role of isopeptidase T. Biochemistry *34*, 14535–14546.

Woolford, C.A., Daniels, L.B., Park, F.J., Jones, E.W., Van Arsdell, J.N., and Innis, M.A. (1986). The PEP4 gene encodes an aspartyl protease implicated in the posttranslational regulation of *Saccharomyces cerevisiae* vacuolar hydrolases. Mol. Cell. Biol. *6*, 2500–2510.

Xiao, W., Fontanie, T., and Tang, M. (1994). UBP5 encodes a putative yeast ubiquitin-specific protease that is related to the human Tre-2 oncogene product. Yeast *10*, 1497–1502.

Yokota, K., *et al.* (1996). cDNA cloning of p112, the largest regulatory subunit of the human 26S proteasome, and functional analysis of its yeast homologue, Sen3p. Mol. Biol. Cell *7*, 853–870.

Yoshimura, T., *et al.* (1993). Molecular characterization of the "26S" proteasome complex from rat liver. J. Struct. Biol. *111*, 200–211.